C. R. Geoscience 350 (2018) 100–109

Contents lists available at ScienceDirect

Comptes Rendus Geoscience

www.sciencedirect.com

Petrology, Geochemistry

Extreme source heterogeneity and complex contamination patterns along the Cameroon Volcanic Line: New geochemical data from the Bamoun plateau

Luc Achille Ziem à Bidias [a,b], Gilles Chazot [c,*], Amidou Moundi [a], Philippe Nonnotte [c]

[a] Département des sciences de la terre et de l'université, Faculté des sciences, Université de Yaoundé-1, BP 812, Yaoundé, Cameroun
[b] Laboratoire de géologie, École normale supérieure, Université de Yaoundé-1, BP 047, Yaoundé, Cameroun
[c] UMR 6538, université de Brest (UBO), Géosciences Océan, Institut universitaire européen de la mer (IUEM), place Nicolas-Copernic, 29280 Plouzané, France

ARTICLE INFO

Article history:
Received 17 October 2017
Accepted after revision 23 November 2017
Available online 22 February 2018

Handled by Marc Chaussidon

Keywords:
Cameroon Volcanic Line
Geochemistry
Mantle source
Crustal contamination
Basalt

ABSTRACT

We investigated mafic and felsic volcanic rocks from the Bamoun plateau, a magmatic province located north of Mount Cameroon, in the continental part of the Cameroon Volcanic Line (CVL). Basalts and dacites were probably emplaced more than 40 Ma ago, while basanites represent very young volcanic eruptions. Among the basalts, some of them have suffered crustal contamination during their uprise through the continental crust, and their primary trace element and isotopic compositions have been slightly modified. The formation of the dacites was also accompanied by some crustal contamination. Non-contaminated rocks show that the oldest magmas are transitional basalts formed by relatively high degrees of partial melting of a moderately enriched mantle source, probably containing pyroxenites. Recent basanites were produced by very low partial melting degrees of an enriched mantle source with HIMU composition, but different from the source of the nearby Mount Cameroon lavas. The mantle beneath the CVL is thus very heterogeneous, and the tendency towards more alkaline mafic-ultramafic compositions in the youngest volcanic manifestations along the CVL seems to be a general feature of all CVL.

1. Introduction and geological setting

The Cameroon Volcanic Line (CVL) is one of the major recent magmatic provinces in Africa (Fitton and Dunlop, 1985). It extends over up to 1500 km from northeast to southwest, with the peculiarity of being partly on the Africa continental crust, and partly on the Atlantic oceanic crust (Fig. 1). The magmatic activity of the CVL also covers a large period of time. Several plutonic massifs as well as some volcanic rocks were emplaced more than 50 Ma ago (Moundi et al., 1996; Okomo Atouba et al., 2016), while the last volcanic activity is the year-2000 eruption of Mount Cameroon. The origin of this large magmatic province is still highly debated. It has been argued that the alignment of the volcanic massifs is the ancient track of the Saint-Helena mantle plume, but no age progression has been evidenced along the CVL. Several alternative models have been proposed, suggesting a formation of the CVL from several mantle plumes (Ngako et al., 2006), or the melting of the uppermost mantle previously impregnated by the Saint-Helena hot spot (Halliday et al., 1988; Lee et al., 1994; Rankenburg et al., 2005). More recently, geophysical

* Corresponding author.
E-mail address: Chazot@univ-brest.fr (G. Chazot).

https://doi.org/10.1016/j.crte.2017.11.004
1631-0713/

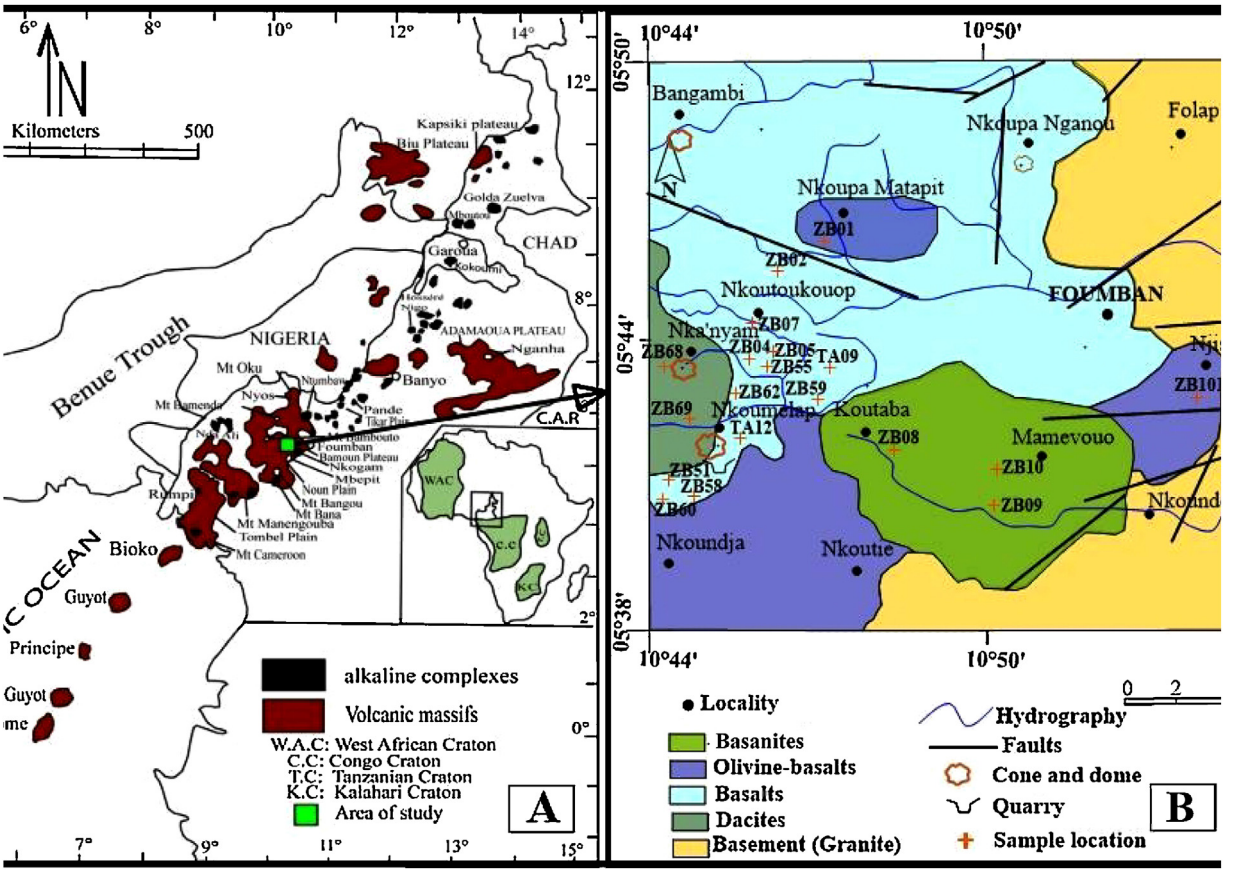

Fig. 1. A. General map of the Cameroon Volcanic Line (CVL), showing the location of the Bamoun plateau. B. Geological map of the studied area showing the location of the samples analyzed in this study.

data as well as numerical modelling have been used to bring more constraints on the structure and evolution of this part of Africa, and the model of mantle melting due to edge-driven convection along the Congo craton has been put forward to explain the linear structure of the CVL as well as its extension on the oceanic plate (Adams et al., 2015; De Plaen et al., 2014; Fourel et al., 2013; Milelli et al., 2012; Reusch et al., 2010, 2011). Even in the framework of these models, there are still many unanswered questions about the composition of the sources of the magmatism, as well as about their location in the mantle beneath the CVL.

We investigated volcanic rocks from the southwestern part of the Bamoun plateau, located in the central part of the continental CVL (Fig. 1). The studied volcanic rocks were emplaced on Pan-African gneisses, granites and gabbros, and both mafic and felsic rocks are present on the field; old basalts appear in deep valleys as part of lava flows, often highly weathered. They are in some places covered by ignimbrite deposits from the Mbam massif nearby. On the opposite, basanites are very fresh volcanic rocks, and form columnar lava flows sitting on top of older volcanic products and appear as the youngest volcanic event in the area. The same field relationships were already described and confirmed by K–Ar dating (Moundi et al., 2007, Okomo Atouba et al., 2016).

Major and trace elements analyses, as well as Sr, Nd, and Pb isotopic measurements were performed on these samples in order to assess the importance of the interactions between the mantle magmas and the crustal rocks, and to discuss the nature and composition of the mantle source of this volcanism, especially in an area where magmatic activity has been present for more than 50 Ma (Moundi et al., 1996; Okomo Atouba et al., 2016), allowing us to discuss the melting process evolution through time. In their previous studies, Moundi et al. (1996, 2007) focused on the oldest volcanic rocks of the area, and did not provide any Pb isotopic data, while the basanites were poorly studied by Okomo Atouba et al. (2016).

2. Analytical techniques

Major and trace elements were obtained by ICP–AES and ICP–MS at IUEM (European Institute for Marine Studies, "Pôle de spectrométrie ocean", Brest, France). Sr and Nd isotopic measurements were performed on a Thermo Scientific Triton at the IUEM in Brest (France), while Pb isotope compositions were obtained using the Thermo Neptune MC–ICP–MS of IFREMER-Brest. The detailed analytical procedures and the analytical results are available as supplementary material.

2.1. Major and trace element analyses

Whole-rock major and some trace elements were measured on the Horiba-Jobin-Yvon® Ultima 2 ICP-AES at the IUEM (European Institute for Marine Studies, Pôle de Spectrométrie Océan, Brest, France). A description of the analytical procedure is given in Cotten et al. (1995). Elements were determined from an H_3BO_3 solution, boron being used as internal standard for ICP-AES analysis. For major elements, relative standard deviation is 1% for SiO_2 and 2% for the other major elements, except for low values (< 0.50 wt.%), for which the absolute standard deviation is ± 0.01 wt.%.

Trace element concentrations were measured with a Thermo Element 2 HR-ICP-MS in Brest (France), after a repeated HF-$HClO_4$ digestion, and HNO_3 dilutions. Details of the analytical procedure are given in Li and Lee (2006). The repeated analysis of the international standard BCR2 demonstrated an external reproducibility better than 5–10% depending on the element and concentration. Major and trace element data are presented in Table 1.

2.2. Sr–Nd–Pb isotopic analyses

Pb isotope compositions were obtained from single HF-HNO3 dissolutions of 500 mg of sample and analysed using the Thermo Neptune MC–ICP–MS of Ifremer-Brest. 2σ internal errors never exceeded the last significant digit (1E-5) in each analysis.

Sr–REE dried fractions, previously collected at the beginning of Pb column separation, were dissolved and dried two times with HNO_3 at 95°C until complete dryness. Dry samples were dissolved again in HCl prior to elution. Chemical separation for Sr and REE was performed on cationic DOWEX® AG50X8 200–400 mesh columns. Sr was kept and proceeded another time in the same column to efficiently separate Sr from Rb and Ca. Nd was further eluted on LnSpec Eichrom resin. Isotopic measurements were performed on a Thermo Scientific Triton at the IUEM in Brest (France). Sr was run on a single W filament with Ta activator, while Nd was run on a Re double filament. International standards were run regularly to check our measurements:

- Sr: NBS987, average value $^{87}Sr/^{86}Sr = 0.710262 \pm 12$ (2σ, $n = 10$);
- Nd: JNdi-1, average value $^{143}Nd/^{144}Nd = 0.512106 \pm 14$ (2σ, $n = 6$);
- La Jolla, average value $^{143}Nd/^{144}Nd = 0.511848 \pm 12$ (2σ, $n = 3$).

Blanks were very low and considered negligible. According to previously published geochronological data and to observations on the field, the Sr and Nd isotopic data on basalts and dacites have been recalculated to 45 Ma initial ratios while the basanites data have not been changed as these rocks are very young. Measured and initial isotopic ratios are presented in Table 1.

3. Petrography and mineralogy

The Bamoun samples are basanites, basalts, and dacites. Phenocrysts are olivine (up to 0.5 mm) and clinopyroxene (up to 3 mm) in the basanites, and clinopyroxene (< 1 mm) and plagioclase (up to 5 mm) in the basalts, with some rare olivine. Dacites (ZB68 and ZB69) are fine-grained microlithic rocks with ghost of what were probably feldspar phenocrysts. The groundmass is made of quartz and feldspar.

In the basalts, the olivine composition ranges from Fo_{53} to Fo_{69}, while it ranges from Fo_{56} to Fo_{79} in the basanites. Clinopyroxenes are augites in basalts ($Wo_{31-45}En_{31-42}Fs_{11-28}$), but are mostly diopsides in basanites ($Wo_{45-52}En_{32-44}Fs_{11-21}$), except some outer rims of micro-phenocrysts with augite composition. According to the classification defined by Leterrier et al. (1982), based on the Ti, Ca, and Na contents, clinopyroxenes from the basanites belong to the "alkali basalts" group, and those analyzed in the basalts define a group clearly belonging to the "tholeiitic basalts". The plagioclases in the basanites are calcic, with anorthite content up to An_{79}, and the composition is richer in Na in the basalts, with anorthite contents ranging from An_{64} to An_{29}. In the dacites, feldspars are rich in K, with a homogeneous composition close to Or_{96}.

4. Geochemical data

4.1. Major elements

In the $Na_2O + K_2O$ vs. SiO_2 TAS classification diagram (Fig. S1, Le Bas et al., 1986), the Bamoun samples define three groups of rocks. Three samples (ZB08, ZB09 and ZB10) are basanites with olivine and nepheline normative composition. A second group is made of basalts with few samples plotting slightly in the basaltic andesite field. All these samples will be referred to as basalts. They are mostly sub-alkaline and contain quartz and hyperstene in their normative composition (except ZB01 and ZB101). The third group comprises two alkali-poor dacites (ZB68 and ZB69).

The basalts have a fairly restricted range in major element composition, with SiO_2 ranging from 47.9 to 52.8 wt% and MgO ranging from 2.8 to 5.1 wt%. The basanites have very different major element compositions, with lower SiO_2, Al_2O_3, and TiO_2, and higher CaO, MgO, P_2O_5, and Na_2O contents than the basalts. Similar chemical compositions were already noticed by Moundi et al. (1996) and Okomo Atouba et al. (2016). As expected, the two dacites have high SiO_2 and K_2O contents, but low CaO, MgO, and TiO_2 concentrations.

4.2. Trace elements

Chondrite-normalized extended incompatible element patterns are shown in Fig. 2. All the Bamoun samples are enriched in LREE and in incompatible elements compared to HREE, but the three groups of samples (basanites, basalts, dacites) display also clearly distinct trace element contents. The basalts have homogeneous REE and trace

Table 1
Measured and initial isotopic ratios for the Bamoun Plateau lavas.

	ZB08	ZB09	ZB10	ZB01	ZB02	ZB04*	ZB05	ZB07	TA09*	TA12*	ZB51	ZB55	ZB58	ZB59	ZB60	ZB62*	ZB101	ZB68	ZB 69
SiO_2	42.7	42.8	42.4	46.6	47.9	47.9	51.6	47.1	51.9	47.5	49.6	50.3	48.7	51.2	48.1	44.5	49.9	65.7	64.8
Al_2O_3	13.2	13.1	12.9	14.8	14.5	13.8	13.8	15.5	13.9	13.5	13.5	13.2	13.7	13.7	12.8	12.3	15.7	13.5	12.8
Fe_2O_3 (t)	13.7	14.0	13.3	14.2	13.6	14.1	13.0	11.9	12.9	14.8	13.8	13.4	13.9	12.1	14.9	13.3	12.4	6.2	5.9
MgO	7.05	7.00	7.05	4.76	3.90	3.45	3.15	4.85	3.44	3.91	3.96	3.57	3.87	3.20	2.62	3.56	4.66	0.49	0.69
CaO	11.71	11.59	11.49	7.50	7.46	7.41	7.49	9.14	7.65	6.57	7.21	7.66	7.92	7.95	7.82	9.18	7.17	2.22	3.59
Na_2O	4.08	4.17	4.25	3.64	3.07	3.19	3.08	2.90	3.22	3.44	2.81	3.13	2.89	3.23	3.05	3.29	3.80	1.45	2.07
K2O	1.45	1.48	1.51	1.21	1.37	0.73	1.64	0.57	1.65	0.70	1.28	1.51	0.86	1.72	0.71	0.76	1.47	4.86	3.65
TiO_2	2.65	2.65	2.58	3.37	3.27	3.14	2.93	2.88	2.89	2.95	3.06	3.03	3.03	2.96	2.65	2.69	2.86	0.54	0.57
P_2O_5	1.265	1.279	1.184	0.913	0.672	0.676	0.725	0.403	0.776	1.098	0.587	0.608	0.586	0.712	0.954	0.948	0.729	0.093	0.119
MnO	0.260	0.267	0.248	0.143	0.177	0.181	0.200	0.167	0.193	0.216	0.206	0.204	0.192	0.196	0.291	0.256	0.142	0.047	0.104
LOI	0.38	0.55	−0.08	2.35	1.79	4.48	2.26	2.72	2.14	7.21	2.77	1.51	3.29	2.36	6.82	8.67	1.70	4.89	5.21
TOTAL	98.46	98.90	96.88	99.49	97.81	99.06	99.88	98.08	100.67	101.88	98.74	98.07	98.86	99.26	100.68	99.51	100.51	99.94	99.51
Li	12.43	14.65	13.20	12.99	7.77		4.29	6.88			14.31		12.64	10.76	20.12		9.21	8.04	
Be	3.47	3.61	3.13	1.99	3.00		2.72	1.82			2.15		2.52	2.94	2.42		3.35	3.14	
Sc*	19.00	18.96	19.62	16.41	20.80	28.50	26.35	23.14	25.82	22.73	27.91	26.82	27.81	26.31	26.35	21.42	15.65	7.18	8.14
V*	205.50	201.84	209.43	200.27	197.57	255.06	213.97	232.79	226.84	149.07	275.84	291.40	299.13	238.02	128.08	149.99	157.98	4.21	4.11
Cr*	128.39	132.78	131.95	43.94	15.60	4.42	4.34	47.57	3.14	8.72	7.75	16.48	4.14	0.37	2.23	4.79	50.14	2.27	0.59
Co*	44.70	42.78	43.85	39.71	38.23	31.39	29.16	62.68	29.27	42.04	35.41	32.83	35.54	30.33	20.99	34.12	38.56	1.60	2.25
Ni*	88.68	90.74	93.80	61.11	37.26	15.56	3.65	118.90	4.85	17.56	19.50	19.57	17.56	6.63	2.62	16.89	68.87	0.58	0.89
Cu	88.57	87.35	82.04	60.51	62.11		38.91	69.89			42.52		41.54	34.08	31.79		46.90	6.71	
Zn	166.26	178.42	163.60	161.82	197.51		170.47	155.59			176.73		164.98	177.50	191.40		186.15	108.61	
Ga	28.03	29.98	28.03	28.13	32.42		30.22	28.30			29.45		31.91	29.58	31.02		32.45	31.04	
Ge	4.57	4.73	4.14	4.01	4.54		4.48	3.12			3.50		4.44	3.74	3.72		4.70	3.78	
Rb	52.59	55.93	51.93	17.73	33.53	18.70	38.67	4.30	30.79	10.81	24.99		8.72	36.21	12.15	13.24	31.51	123.44	
Sr	1312.8	1396.3	1267.3	577.6	658.9	552.3	614.2	502.2	569.8	474.0	544.4	481.0	590.5	590.9	610.4	494.2	627.4	137.3	154.1
Y	43.07	42.33	40.78	35.06	50.36	39.91	50.42	38.81	41.07	46.82	42.46	36.03	40.70	44.38	49.62	48.17	45.78	59.03	59.75
Zr	387.0	445.4	397.2	285.5	409.9	303.3	417.4	236.8	288.9	300.9	347.2	301.9	291.5	375.9	305.6	279.5	507.0	880.8	846.1
Nb	163.17	178.57	163.19	39.64	42.96	23.04	31.35	29.63	24.64	32.58	27.43	23.59	26.52	31.58	37.70	30.44	58.39	59.90	47.79
Cs	0.45	0.59	0.61	0.66	0.45		1.93	0.09			0.30		0.08	0.40	0.18		0.16	0.47	
Ba	968.0	1024.8	934.6	299.0	876.6	1410.8	1034.0	238.0	870.6	610.7	811.5	737.9	554.3	822.1	439.7	523.7	314.3	2002.9	1426.5
La	100.59	107.94	93.70	29.89	36.89	36.07	37.47	18.25	39.13	32.68	32.03	33.95	32.48	35.33	36.01	34.50	35.91	67.22	57.24
Ce	212.89	214.25	194.95	69.57	86.79	75.10	86.99	42.68	85.40	75.00	72.89	73.46	76.50	87.01	90.13	79.75	95.32	133.14	115.13
Pr	21.11	21.24	18.09	8.45	10.89		9.97	5.60			9.25		8.75	10.70	10.38		12.19	15.81	
Nd	75.06	78.49	66.06	37.08	44.05	46.06	41.42	25.10	47.81	48.44	38.63	43.13	39.48	42.42	43.45	50.54	51.53	65.19	59.77
Sm	12.43	13.08	11.64	8.28	10.25	9.83	9.20	6.43	10.61	11.82	8.15	9.80	8.30	9.01	9.85	11.33	11.20	12.52	13.25
Eu	3.93	4.37	3.86	2.55	3.09	3.25	3.20	1.90	3.24	4.49	3.08	3.17	2.59	3.09	3.64	4.71	3.63	3.28	3.73
Gd	11.30	11.88	10.31	8.24	10.27	9.84	8.96	6.65	9.32	11.93	8.22	8.40	8.42	9.11	10.37	11.98	10.13	11.85	12.37
Tb	1.53	1.50	1.37	1.09	1.42		1.36	1.00			1.32		1.17	1.31	1.46		1.46	1.86	
Dy	7.25	7.39	6.25	5.83	7.98	7.35	7.10	5.31	7.71	9.37	6.38	6.95	6.08	7.01	7.69	9.34	7.28	10.55	10.54
Ho	1.14	1.16	1.09	0.94	1.31		1.29	1.03			1.17		1.16	1.30	1.41		1.21	1.96	
Er	2.98	2.90	2.73	2.34	3.60	3.52	3.37	3.09	3.78	4.10	2.99	3.46	2.86	3.15	3.67	4.38	3.00	5.44	5.20
Tm	0.37	0.37	0.36	0.31	0.44		0.48	0.38			0.40		0.41	0.46	0.49		0.36	0.79	
Yb	2.19	2.34	2.00	1.75	2.98	3.20	2.75	2.27	3.18	3.15	2.37	2.98	2.31	2.82	2.83	3.36	1.99	4.97	5.20
Lu	0.31	0.34	0.29	0.24	0.40		0.39	0.32			0.37		0.36	0.40	0.40		0.28	0.73	
Hf	5.64	5.77	5.55	4.78	6.87		6.45	4.23			5.92		4.40	6.24	4.86		8.30	16.74	
Ta	6.42	6.69	6.12	1.79	1.94		1.41	1.33			1.24		1.25	1.45	1.63		2.64	3.23	
Tl	0.07	0.07	0.06	0.09	0.30		0.42	0.04			0.16		0.07	0.28	0.12		0.07	1.57	
Pb	5.18	5.15	5.34	1.74	4.06		6.66	1.95			5.06		4.96	6.81	3.50		2.05	15.53	
Th	9.57	9.63	8.57	1.78	2.06	3.77	3.59	1.26	4.08	2.71	2.55	3.25	2.41	2.99	1.65	2.64	2.67	8.74	10.43
U	2.90	2.87	2.69	0.67	0.64		0.98	0.42			0.66		0.70	0.86	0.50		0.94	2.49	

Table 1 (*Continued*)

	ZB08	ZB09	ZB10	ZB01	ZB02	ZB04*	ZB05	ZB07	TA09*	TA12*	ZB51	ZB55	ZB58	ZB59	ZB60	ZB62*	ZB101	ZB68	ZB 69
Elements analyzed by ICP–AES																			
$^{87}Sr/^{86}Sr$	0.70352		0.70356	0.70407	0.70480		0.70641	0.70464			0.70545		0.70537	0.70569			0.70350	0.70721	
$^{143}Nd/^{144}Nd$	0.512892		0.512885	0.512735	0.512393		0.512350	0.512716			0.512354		0.512301	0.512288			0.512851	0.512546	
$^{206}Pb/^{204}Pb$	19.829		19.813	18.636	16.694		17.485	18.531			17.182		16.997	17.108			19.631	18.031	
$^{207}Pb/^{204}Pb$	15.653		15.653	15.539	15.337		15.479	15.588			15.426		15.404	15.419			15.643	15.530	
$^{208}Pb/^{204}Pb$	39.489		39.489	38.575	36.589		37.777	38.867			37.284		37.068	37.196			39.454	38.535	
$^{87}Sr/^{86}Sri$	0.70352		0.70356	0.70401	0.7047		0.70629	0.70462			0.70537		0.70534	0.70558			0.7034	0.70555	
$^{143}Nd/^{144}Nd_i$	0.512892		0.512885	0.512695	0.512352		0.512310	0.512670			0.512316		0.512264	0.512250			0.512812	0.512512	

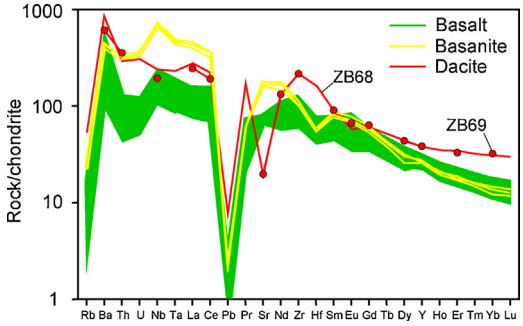

Fig. 2. Chondrite-normalized trace element patterns for the Bamoun lavas, showing an enrichment in some incompatible elements of the basanites compared to the basalts. Normalization values from Anders and Grevesse (1989).

element compositions, with a slight enrichment in LREE over HREE, with La/Yb_N ratios ranging from 7.1 to 13. A few samples show a small positive Eu anomaly. The three basanites are very homogeneous in REE, with steeper patterns than the basalts. They have similar HREE but higher LREE concentrations, with La/Yb_N ratio = 32. Dacites have flatter REE patterns with a higher HREE content than the mafic rocks, but an LREE content intermediate between the basalts and the basanites. Their La/Yb_N ratio ranges from 7.6 to 9.4, and they have a slight negative Eu anomaly.

When considering all the trace elements, the basanites confirm that they are highly enriched in incompatible elements, with very high Th, U, Nb, Ta, and Sr contents as well as higher Zr content than the basalts for similar Hf content. The basalts have low Th and U concentrations and very variable Rb and Ba contents. The dacites have a contrasted trace element pattern, with the highest Ba, Zr and Hf concentrations, but lower Th, U, Nb, and Ta contents than the basanites. They have a very pronounced Sr negative anomaly, probably reflecting some amount of plagioclase fractionation.

4.3. Isotopes

From the morphology observed on the field, it is clear that the basanites represent a very recent volcanic episode, while the basalts and the dacites were emplaced long time ago. In agreement with the K–Ar ages previously reported for the old volcanic episodes in the area (Moundi et al., 2007; Okomo Atouba et al., 2016), we calculated initial Sr and Nd isotopic compositions back to 45 Ma for the basalts and the dacites. The Bamoun samples cover a large range in Sr and Nd compositions (Fig. 3), with $^{87}Sr/^{86}Sr_i$ ranging from 0.7034 to 0.7063 and $^{143}Nd/^{144}Nd_i$ from 0.51225 to 0.51281 for the basalts. The basanites have very restricted isotopic compositions with $^{87}Sr/^{86}Sr$ ranging from 0.70352 to 0.70356 and $^{143}Nd/^{144}Nd$ from 0.512885 to 0.512892. The analyzed dacite has a high $^{87}Sr/^{86}Sr_i$ ratio (0.70555) and $^{143}Nd/^{144}Nd_i$ intermediate (0.512512) between the most and the less radiogenic basalts.

Similar observations can be made for the Pb isotopic ratios, with the highest and very restricted isotopic ratios for the basanites (for example $^{206}Pb/^{204}Pb$ from 19.812 to 19.828), while the basalts cover a larger range of isotopic

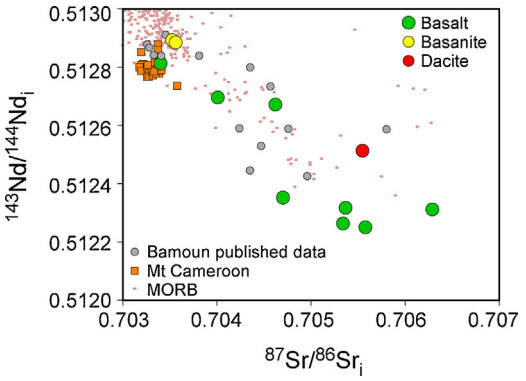

Fig. 3. $^{143}Nd/^{144}Nd_i$ vs. $^{87}Sr/^{86}Sr_i$ diagram. The Bamoun lavas are compared to the previously published data from the Bamoun plateau (Moundi et al., 2009; Okomo Atouba et al., 2016), but also to the data from Mount Cameroon (Ballentine et al., 1997; Halliday et al., 1988; Tsafack et al., 2009; Yokoyama et al., 2007). MORB data are from the GEOROC database.

compositions, with $^{206}Pb/^{204}Pb$ ranging from 16.694 to 19.631 (Fig. 6). As for Nd, the dacite has Pb isotopic composition intermediate between the less and the most radiogenic basalts, with $^{206}Pb/^{204}Pb = 18.031$.

5. Discussion

The nature and composition of the mantle sources is a pivotal question in the understanding of the CVL and is still highly debated. All the available data on the CVL magmatism point towards highly heterogeneous sources for the magmas, but the location and origin of these sources are still debated. Furthermore, the youngest volcanic massif along the CVL is represented by Mount Cameroon, and several studies pointed out that the source of the Mount Cameroon magmas has a different composition compared to the mantle from which the oldest part of the CVL magmas originate. Whether this difference is due to the age of the volcanism or to the fact that Mount Cameroon lies close to the ocean–continent boundary is also a very important question.

One important aspect of the studies of the mantle sources of continental magmatism is to assess how important are the interactions between the mantle magmas and the rocks from the continental crust during the ascent and storage of the magmas. This contamination process has often been underestimated in many studies concerning CVL magmatism, even if several papers have underlined its importance (Gannoun et al., 2015; Halliday et al., 1988; Kamgang et al., 2007, 2008, 2013; Marzoli et al., 1999; Okomo Atouba et al., 2016; Rankenburg et al., 2005; Tchuimegnie Ngongang et al., 2015).

5.1. Crustal contamination

The three basanites are very rich in incompatible trace elements, and are very difficult to contaminate by crustal products. They have very low silica content ($SiO_2 < 44$ wt%), which makes unlikely their interaction with high silica crustal melts, in agreement with their very unradiogenic Sr isotopic composition. At the opposite, the basalts have higher silica content and a large range in isotopic compositions. Their SiO_2 content is strongly correlated with Sr and Nd isotopic ratios, with increasing Sr (Fig. S2) and decreasing Nd isotopic values for increasing SiO_2. These correlations are clear indicator that, during their differentiation, the mafic magmas have interacted with high silica rocks with more radiogenic Sr and less radiogenic Nd compositions, similar to what expected from rocks from the continental crust.

Nb is highly depleted in all continental crust rocks (Taylor and McLennan, 1985) and the La/Nb ratio is often used as an indicator of crustal contamination. La/Nb ratio is correlated with Sr, Nd and Pb isotopic ratios for the Bamoun basalts and this indicates interactions with a crustal component with low Pb isotopic ratios. However, some basalts (ZB01, ZB07 and ZB101) have isotopic composition different from the basanites, but with similar and low La/Nb ratio. For these samples, their different isotopic composition reflects differences in the composition of the mantle source. A detailed study of this contamination process shows that it affected selectively some elements like Ba and Nb, but Th and the REE were not modified by the contamination. The contaminated samples will be identified with special symbols in all the isotopic diagrams discussing the origin of the Bamoun volcanic rocks.

5.2. Mantle sources

In the Ni vs. Th diagram (Fig. 4), all the analyzed mafic samples have Ni concentrations lower than 120 ppm, and are clearly not primary magmas in equilibrium with mantle minerals. Two trends compatible with olivine fractionation are visible, one with $Th < 4$ ppm with all the basalts and some already published data from the Bamoun area, and another one with higher Th content, with the basanites, a few published data from the literature, and overlapping with the data from the Mount Cameroon lavas. These two trends point towards two different chemical compositions for their primary magma, one with low Th concentration, probably lower than 2 ppm, and the other one with a much more enriched composition.

The Th/La ratio is strongly correlated with the different isotope ratios and, when plotted against $^{206}Pb/^{204}Pb$, two different groups defined two parallel correlations (Fig. 5). One group comprises all the basalts but three and the dacite, and defines a positive correlation on the low Pb isotopic ratio of the diagram. The second group defines a nearly parallel positive correlation, but with higher Pb isotopic ratios, and comprises the basanites and the three basalts ZB01, ZB07, and ZB101, for which no or negligible crustal contamination has been observed. Samples from Mount Cameroon extend this trend towards higher values of $^{206}Pb/^{204}Pb$. Clearly most of the basalts as well as the dacites have been shifted from the main trend towards low Pb isotopic values for similar Th/La ratio during the crustal contamination process. These correlations clearly highlight a mixing between at least two different mantle sources beneath the CVL. One source has high Pb and low Sr isotopic ratios. On the other side of this correlation, the

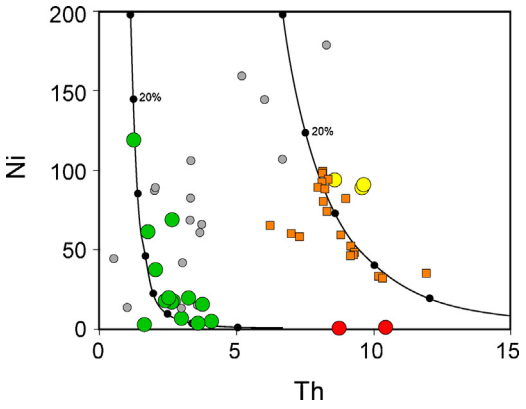

Fig. 4. Ni vs. Th diagram. Two groups of samples are clearly visible, one made of basalts, while the other one contains the basanites and the rocks from Mount Cameroon. Data of Mount Cameroon from Déruelle et al. (2000), Suh et al. (2008), and Okomo Atouba et al. (2016). Same symbols as in Fig. 3. The two black lines represent very simple models of olivine fractionation starting from a primary magma with 300 ppm Ni and 1 ppm or 6 ppm Th. Partition coefficients for Ni and Th between olivine and silicate magma are set to 5 and 0.0001, respectively. The black dots on the models represent 10% increment of olivine fractionation.

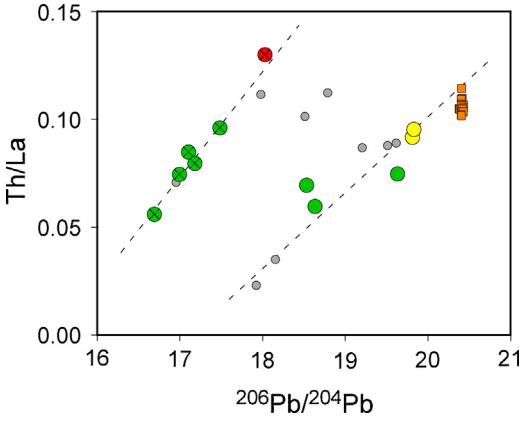

Fig. 5. Th/La vs. $^{206}Pb/^{204}Pb$ diagram for the Bamoun and the Mount Cameroon volcanic rocks. Two different trends are clearly visible and highlight the role of crustal contamination. Mount Cameroon data from Yokoyama et al. (2007). The symbols with a cross represent the contaminated samples, identified using all the geochemical tools available. Same symbols as in Fig. 3. The dashed lines are only indicative trends.

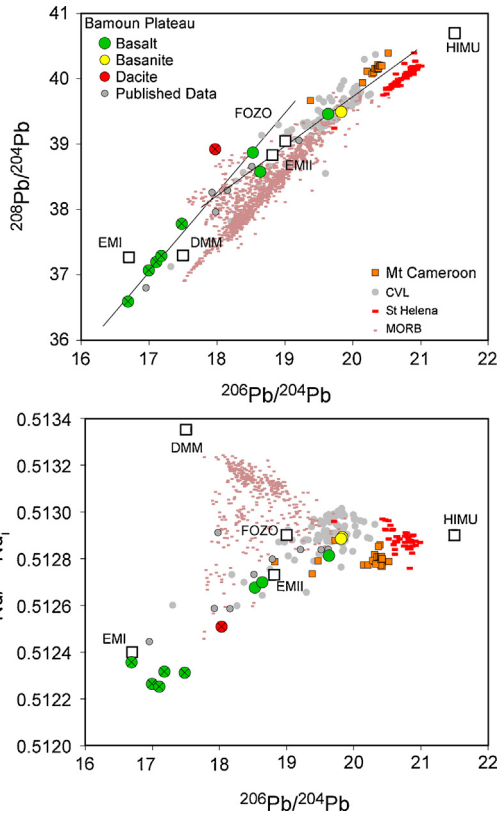

Fig. 6. $^{208}Pb/^{204}Pb$ vs. $^{206}Pb/^{204}Pb$ and $^{143}Nd/^{144}Nd_i$ vs. $^{206}Pb/^{204}Pb$ diagrams for the Bamoun lavas, showing, for the Pb isotopes, two lines of mixing between different components (see text for more detailed explanations). For the Cameroon Volcanic Line (CVL), only mafic rocks are represented. Data from Mount Cameroon are from Halliday et al. (1988), Ballentine et al. (1997), Yokoyama et al. (2007) and Tsafack et al. (2009). Data for the CVL are from Halliday et al. (1988), Ballentine et al. (1997), Rankenburg et al. (2005), Asaah et al. (2015), Tchuimegnie Ngongang et al. (2015), and Kamgang et al. (2013). MORB and Saint-Helena data are from the GEOROC database. The white boxes are the main mantle components defined by Zindler and Hart (1986). The symbols with a cross represent the contaminated samples, identified using all the geochemical tools available.

second mantle source has low Pb isotopic composition, higher Sr isotopic ratio, and low Th content. The dacites plot on the same correlation as the contaminated basalts and have similar La/Yb ratios, indicating that they were formed by crystal fractionation and assimilation from the basaltic magmas.

Large differences in the La/Yb ratio between the basalts, the basanites and the Mount Cameroon samples can be ascribed either to different partial melting rates or to mantle source heterogeneities. When combined with Th/La, these two trace element ratios provide key information about the mantle processes at the origin of the CVL mafic magmas (Fig. S3). The whole data for the mafic lavas from the CVL cover a quite restricted range of Th/La ratios, with values ranging from 0.8 to 0.14 for most of the samples. This small range is quite surprising as the plotted data represent a large number of mafic rocks covering the whole continental part of the CVL with magmas emplaced from more than 40 Ma ago to the present-day Mount Cameroon eruptions. It implies that from the point of view of trace elements, source heterogeneities are rather limited in the mantle beneath the CVL. The basalts from the Bamoun plateau have among the lowest Th/La ratios of the CVL, while the basanites plot at the middle of the range. Variations of the La/Yb ratio are larger, with values ranging from less than 10 up to 47. Most of these variations can be ascribed to various partial melting degrees, even if source heterogeneities can also add to this variability. Interestingly, the mafic rocks of the Bamoun plateau have the most extreme La/Yb ratios, with basalts having whole CVL values among the lowest ones, while basanites have the highest La/Yb ratios. Clearly, the degree of partial melting has

changed dramatically beneath this area of the CVL from 45 Ma to the present day. This is also well illustrated in a zoom of the mafic part of the classical TAS diagram (Fig. S4). A large majority of the mafic samples from the CVL plot on the alkali part of the diagram, above the dividing lines defined by Irvine and Baragar (1971) and Bellieni et al. (1982). Moundi et al. (1996) already analyzed some mafic rocks from the Bamoun plateau with transitional affinity, and this is well confirmed by our new data. The mafic rocks from the Bamoun plateau are once more divided into two extreme groups, with basanites having the more alkali composition among the rocks of the CVL, while basalts plot on the lower right of the diagram, entirely into the transitional and sub-alkaline domains. Considering that the basalts are clearly older than the basanites, the melting regime in the mantle changed dramatically beneath the Bamoun plateau to form transitional basalts older than 40 Ma old and more alkali-rich basanites, more recently.

The isotopic ratios of mafic rocks from the CVL cover a limited range of compositions in Sr, Nd, and Pb, and part of the variability is probably due to small amounts of crustal assimilation. Our new Bamoun data plot in the middle of this range (Fig. 6 and Fig. S5), except for some samples with very low Pb isotopic ratios, which have been affected by crustal contamination, as already shown in the same area by Moundi et al. (2009) and Okomo Atouba et al. (2016). Interestingly, the Mount Cameroon mafic rocks have isotopic compositions that do not overlap with those of other CVL samples, with higher Pb isotopic ratios. These Mount Cameroon compositions are also different from those of the mafic rocks from Saint-Helena Island, and this observation is against some ideas that the source of the CVL magmas is similar to the mantle plume at the origin of this island and represents the old track of the Saint-Helena mantle plume. In the Pb isotopic spaces, where mixing between different mantle sources defines straight lines, the non-contaminated Bamoun samples define a trend compatible with a mixing between two different sources, one with low Pb isotopic compositions, but also low Nd and high Sr isotopic ratios and pointing towards FOZO and EMI compositions, and a second one with higher Pb isotopic composition pointing towards a HIMU mantle reservoir. Two important observations can be added for the understanding of the origin and nature of the mantle sources beneath the CVL:

- the isotopic trends defined by the Bamoun mafic rocks, but also by the majority of the CVL mafic rocks, do not point towards the MORB compositions and the DMM mantle component. The asthenospheric mantle is not (or very slightly) participating to the genesis of the magmas beneath the CVL;
- towards high Pb isotopic values, the isotopic trends defined by the Bamoun mafic rocks do no point towards Saint-Helena basaltic compositions, nor to Mt Cameroon isotopic values.

This confirms that the magmatism of the CVL is not related to the Saint-Helena hotspot track, but also that Mount Cameroon has a peculiar mantle source composition, which is not an end-member of the mixing trend defined by the whole CVL magmas.

The isotopic trend shown by our new Bamoun data, and the already published data from this area, are consistent with a two end-member mixing between two different mantle sources with very contrasted compositions. These two sources are located in the subcontinental lithospheric mantle, and the participation of the asthenosphere is clearly very minor. Okomo Atouba et al. (2016) showed that the EMI-type mantle source produces some basalts with a clear positive Eu anomaly and interpreted this feature as an evidence for the presence of pyroxenitic lithologies in this part of the mantle. This kind of small positive anomaly is present in some of our new Bamoun basalts (e.g., ZB51, ZB60, ZB62) and confirms that pyroxenites probably participated in the genesis of some magmas beneath the CVL. These basalts also have the lowest La/Yb ratios and accordingly are generated by the highest partial melting degrees, which is consistent with the lower melting temperature for pyroxenite lithologies (Hirschmann and Stolper, 1996). On the opposite, the basanites with the highest Pb isotopic ratios point toward the HIMU-like mantle component, and have the highest La/Yb ratios and are also highly enriched in the most incompatible elements (Fig. 2). They are generated in a different mantle source, highly enriched in incompatible elements, and by lower partial melting degrees. However, while having high Pb isotopic composition, their mantle source is different from the Mount Cameroon mantle source, and they are formed by even lower partial melting degrees than the Mount Cameroon basalts.

6. Conclusion

The Bamoun plateau records the longest magmatic history of the CVL with some of the oldest mafic rocks analyzed along the volcanic line (more than 50 Ma old, Moundi et al., 1996; Okomo Atouba et al., 2016) up to very recent volcanic eruptions. It also records the largest variations in chemical compositions, with among the most transitional basalts up to the highest alkali- and trace-element-enriched basanites. Although we still need more samples and a more detailed chronology, it is clear that there is a shift with time in the chemistry of the magma formed beneath this part of the CVL, from transitional basalts for the earliest magmatic episodes, formed through high partial melting degrees of a slightly enriched source containing some amount of pyroxenitic lithologies, towards alkali-rich basanites formed by very low partial melting degrees of a highly enriched mantle source with an HIMU affinity, but different from the source of the Mount Cameroon magmas. This tendency towards more alkali basalts in the youngest volcanic manifestations along the CVL seems to be a more general feature for all the CVL, but needs to be investigated in more details.

Acknowledgements

This work is dedicated to Professor Pierre Wandji, who initiated this study but sadly disappeared before its

achievement. Céline Liorzou, Bleuenn Guéguen, and Kévin Quessette are thanked for their help in the acquisition of chemical results. Thanks also to Michel Grégoire and Andrea Marzoli, who provided constructive reviews.

Appendix A. Supplementary data

Supplementary data associated to this article can be found in the online version, at https://doi.org/10.1016/j.crte.2017.11.004.

References

Anders, E., Grevesse, N., 1989. Abundances of the elements: meteoritic and solar. Geochim. Cosmochim. Acta 53, 197–214.

Adams, A.N., Wiens, D.A., Nyblade, A.A., Euler, G.G., Shore, P.J., Tibi, R., 2015. Lithospheric instability and the source of the Cameroon Volcanic Line: evidence from Rayleigh wave phase velocity tomography. J. Geophys. Res. 120, 1708–1727.

Asaah, A.N., Yokoyama, T., Aka, F.T., Usui, T., Kuritani, T., Wirmvem, M.J., Iwamory, H., Fozing, E.M., Tamen, J., Mofor, G.Z., Ohba, T., Tanyleke, G., Hell, J.V., 2015. Geochemistry of lavas from maar-bearing volcanoes in the Oku Volcanic Group of the Cameroon Volcanic Line. Chem. Geol. 406, 55–69.

Ballentine, C.J., Lee, D.C., Halliday, A.N., 1997. Hafnium isotopic studies of the Cameroon Line and new HIMU paradoxes. Chem. Geol. 139, 111–124.

Bellieni, G., Justin Visentin, E., Le Maitre, R.W., Piccirillo, E.M., Zanettin, B., 1983. Proposal for a division of the basaltic field of the TAS diagram. IUGS Subcommission on the Systematics of Igneous Rocks. Circular No. 38. Contribution No. 102. .

De Plaen, R.S.M., Bastow, I.D., Chambers, E.L., Keir, D., Gallacher, R.J., Keane, J., 2014. The development of magmatism along the Cameroon Volcanic Line: evidence from seismicity and seismic anisotropy. J. Geophys. Res. 119, 4233–4252, http://dx.doi.org/10.1002/2013JB010583.

Déruelle, N., Bardintzeff, J.-M., Cheminée, J.-L., Ngounouno, I., Lissom, J., Nkoumbou, C., Etamé, J., Hell, J.-V., Tanyleke, G., N'ni, J., Ateba, B., Ntepe, N., Nono, A., Wandji, P., Fosso, J., Nkouathio, D.G., 2000. Eruptions simultanées de basalte alcalin et de hawaiite au mont Cameroun (28 mars–17 avril 1999). C. R. Acad. Sci. Paris, Ser. IIa 331, 525–531.

Fitton, J.G., Dunlop, H.M., 1985. The Cameroon Line. West Africa and its bearing on the origin of oceanic and continental alkalic basalt. Earth Planet. Sci. Lett. 72, 23–38.

Fosso, J., Ménard, J.-J., Bardintzeff, J.-M., Wandji, P., Tchoua, F.M., Bellon, H., 2005. Les laves du mont Bangou: une première manifestation volcanique éocène à affinité transitionnelle, de la ligne du Cameroun. C. R. Geoscience 337, 315–325.

Fourel, L., Milelli, L., Jaupart, C., Limare, A., 2013. Generation of continental rifts, basins, and swells by lithosphere instabilities. J. Geophys. Res. Solid Earth 118, 3080–3100, http://dx.doi.org/10.1002/jgrb.50218.

Gannoun, A., Burton, K.W., Barfod, D.N., Schiano, P., Vlastélic, I., Halliday, A.N., 2015. Resolving mantle and magmatic processes in basalts from the Cameroon volcanic line using the Re–Os isotope system. Lithos, 224–225, [1–12].

Halliday, A.N., Dickin, A.P., Fallick, A.E., Fitton, J.G., 1988. Mantle dynamics: a Nd, Sr, Pb and O isotopic study of the Cameroon line volcanic chain. J. Petrol. 29, 181–211.

Hirschmann, M.M., Stolper, E.M., 1996. A possible role for garnet pyroxenites in the origin of the 'garnet signature' in MORB. Contrib. Mineral. Petrol. 124, 185–208.

Irvine, T.N., Baragar, W.R.A., 1971. A guide to the chemical classification of the common volcanic rocks. Can. J. Earth. Sci. 523–548.

Itiga, Z., Bardintzeff, J.-M., Wotchoko, P., Wandji, P., Bellon, H., 2013. Tchabal Gangdaba massif in the Cameroon Volcanic Line: a bimodal association. Arabian J. Geosciences 7, 4641–4664.

Kamgang, P., Njonfang, E., Chazot, G., Tchoua, F.M., 2007. Géochimie et géochronologie des laves felsiques des monts Bamenda (ligne volcanique du Cameroun). C R Geoscience 339, 659–666.

Kamgang, P., Chazot, G., Njonfang, E., Tchoua, F.M., 2008. Geochemistry and geochronology of mafic rocks from Bamenda Mountains (Cameroon): source composition and crustal contamination along the Cameroon Volcanic Line. C R Geoscience 340, 850–857.

Kamgang, P., Chazot, G., Njonfang, E., Ngongang, N.B.T., Tchoua, F.M., 2013. Mantle sources and magma evolution beneath the Cameroon Volcanic Line: geochemistry of mafic rocks from the Bamenda Mountains (NW Cameroon). Gondwana Res. 24, 727–741.

Kuepouo, G., Tchouankoue, J.-P., Nagao, T., Sato, H., 2006. Transitional tholeiitic basalts in the Tertiary Bana volcano-plutonic complex. Cameroon Line. J. Afr. Earth Sci. 45, 318–332.

Le Bas, M.J., Le Maitre, R.W., Streckeisen, A., Zanettin, B., 1986. A chemical classification of volcanic rocks based on the total alkali-silica diagram. J. Petrology 27, 745–750.

Lee, D.C., Halliday, A.N., Fitton, J.G., Poli, G., 1994. Isotopic variation with distance and time in the volcanic islands of the Cameroon Line, evidence from mantle plume origin. Earth Planet. Sci. Lett. 124, 119–138.

Leterrier, J., Maury, R.C., Thonon, P., Girard, D., Marchal, M., 1982. Clinopyroxene composition as a method of identification of the magmatic affinities of paleo-volcanic series. Earth Planet. Sci. Lett. 59, 139–154.

Li, Z.X.A., Lee, C.T.A., 2006. Geochemical investigation of serpentinized oceanic lithospheric mantle in the Feather River Ophiolite, California: implications for the recycling rate of water by subduction. Chem. Geol. 235, 161–185.

Marzoli, A., Renne, P.R., Piccirillo, E.M., Francesca, C., Bellieni, G., Melfi, A.J., N'ni, J., 1999. Silicic magmas from the continental Cameroon Volcanic Line (Oku, Bambouto and Ngaoundere): ^{40}Ar ^{39}Ar dates, petrology, Sr–Nd–O isotopes and their petrogenetic significance. Contrib. Mineral. Petrol. 135, 133–150.

Mbassa, B.J., Njonfang, E., Benoit, M., Kamgang, P., Grégoire, M., Duchene, S., Brunet, P., Ateba, B., Tchoua, F.M., 2012. Mineralogy, geochemistry and petrogenesis of the recent magmatic formations from Mbengwi, a continental sector of the Cameroon Volcanic Line (CVL), Central Africa. Mineral. Petrol. 106, 217–242.

Milelli, L., Fourel, L., Jaupart, C., 2012. A lithospheric instability origin for the Cameroon Volcanic Line. Earth Planet Sci. Lett. 335–336 [80–87].

Moundi, A., Menard, J.J., Reusser, E., Tchoua, F., Dietrich, V.J., 1996. Découverte de basaltes transitionnels dans le secteur continental de la ligne du Cameroun (massif du Mbam, Ouest-Cameroun). C. R. Acad. Sci. Paris, Ser. IIa 322, 831–837.

Moundi, A., Wandji, P., Bardintzeff, J.-M., Ménard, J.J., Okomo Atouba, L.C., Mouncherou, O.F., Reusser, E., Bellon, H., Tchoua, F.M., 2007. Les basaltes éocènes à affinité transitionnelle du plateau Bamoun, témoins d'un réservoir mantellique enrichi sous la Ligne Volcanique du Cameroun. C. R. Geoscience 339, 396–406.

Moundi, A., Wandji, P., Ghogomu, R.T., Bardintzeff, J.-M., Njilah, I.K., Foumboure, I., Ntieche, B., 2009. Existence of Quaternary ankaramites among Tertiary floods basalts at Koutaba (Bamoun plateau Western Cameroon): petrology and isotope data. Rev. Bulgarian geol. Soc. 70, 115–124.

Ngako, V., Njonfang, E., Aka, F.T., Affaton, P., Nnange, J.M., 2006. The north–south Paleozoic to Quaternary trend of alkaline magmatism from Niger–Nigeria to Cameroon: complex interaction between hotspots and Precambrian faults. J. Afr. Earth Sci. 45, 241–256.

Ngounouno, I., Déruelle, B., Demaiffe, D., 2000. Petrology of the bimodal Cenozoic volcanism of the Kapsiki plateau (northernmost Cameroon Central Africa). J. Volcanol. Geotherm. Res. 102, 21–44.

Ngounouno, I., Déruelle, B., Montigny, R., Demaiffe, D., 2006. Les camptonites du mont Cameroun, Cameroun, Afrique. C. R. Acad. Sci. Paris, Ser. IIa 338, 537–544.

Nkouandou, O.F., Ngounouno, I., Déruelle, B., Ohnenstetter, D., Montigny, R., Demaiffe, D., 2008. Petrology of the Mio-Pliocene volcanism to the north and east of Ngaoundéré (Adamawa Cameroon). C. R. Geoscience 340, 28–37.

Okomo Atouba, L.C., Chazot, G., Moundi, A., Agranier, A., Bellon, H., Nonnotte, P., Kankeu, B., 2016. Mantle sources beneath the cameroon volcanic line: geochemistry and geochronology of the Bamoun plateau mafic rocks. Arabian J. Geosci. 9 (4), 270.

Pouclet, A., Dongmo, A.K., Bardintzeff, J.-M., Wandji, P., Tagheu, P.C., Nkouathio, D., Bellon, H., Ruffet, G., 2014. The Mount Manengouba, a complex volcano of the Cameroon Line: volcanic history, petrological and geochemical features. J. Afr. Earth Sci. 97, 297–321.

Rankenburg, K., Lassiter, J.C., Brey, G., 2005. The role of continental crust and lithospheric mantle in the genesis of Cameroon volcanic line lavas: constraints from isotopic variations in lavas and megacrysts from the Biu and Jos Plateaux. J. Petrol. 46, 169–190.

Reusch, A.M., Nyblade, A.A., Wiens, D.A., Shore, .P.J., Ateba, B., Tabod, C.T., Nnange, J.M., 2010. Upper mantle structure beneath Cameroon from body wave tomography and the origin of the Cameroon Volcanic Line. Geochem. Geophys. Geosyst 11 , http://dx.doi.org/10.1029/2010GC003200.

Reusch, A., Nyblade, A., Tibi, R., Wiens, D., Shore, P., Bekoa, A., Tabod, C., Nnange, J., 2011. Mantle transition zone thickness beneath Came-

roon: evidence for an upper mantle origin for the Cameroon Volcanic Line. Geophys. J. Int. 18, 1146–1150.
Suh, C.E., Luhr, J.F., Njome, M.S., 2008. Olivine-hosted glass inclusions from scoriae erupted in 1954–2000 at Mount Cameroon volcano. West Africa. J. Volcanol. Geotherm. Res. 169, 1–33.
Taylor, S.R., McLennan, S.M., 1985. The continental crust: its composition and evolution. Blackwell Scientific Publications, Oxford312p.
Tchuimegnie Ngongang, N.B., Kamgang, P., Chazot, G., Agranier, A., Bellon, H., Nonnotte, P., 2015. Age, geochemical characteristics and petrogenesis of Cenozoic intraplate alkaline volcanic rocks in the Bafang region, West Cameroon. J. Afr. Earth Sci. 102, 218–232.
Tsafack, J.P.F., Wandji, P., Bardintzeff, J.-M., Bellon, H., Guillou, H., 2009. The Mount Cameroon stratovolcano (Cameroon Volcanic Line Central Africa): petrology, geochemistry, isotope and age data. Mineral. Petrol. 47, 65–78.
Wandji, P., Wotchoko, P., Bardintzeff, J.-M., Bellon, H., 2010. Late Tertiary and Quaternary alkaline volcanism in the western Noun Plain (Cameroon Volcanic Line): New K–Ar ages, petrology and isotope data. Geochem. Mineral. Petrol. Sofia 48, 67–94.
Wotchoko, P., Wandji, P., Bardintzeff, J.-M., Bellon, H., 2005. Données pétrologiques et géochronologiques nouvelles sur le volcanisme alcalin néogène à récent de la rive ouest du Noun (plaine du Noun, Ligne du Cameroun). Rev. Bulgarian Geol. Soc. 66 (1–3), 97–105.
Yokoyama, T., Festus Aka, T., Kusakabe, M., Nakamura, E., 2007. Plume-lithosphere interaction beneath Mt. Cameroon volcano. West Africa: constraints from ^{238}U-^{230}Th ^{226}Ra and Sr–Nd–Pb isotope systematics. Geochim. Cosmochim. Acta 71, 1835–1854.
Zindler, A., Hart, S., 1986. Chemical geodynamics. Annu. Rev. Earth Planet. Sci. 14, 493–571.